

# Fast directional continuous spherical wavelet transform algorithms

J. D. McEwen, M. P. Hobson, D. J. Mortlock, A. N. Lasenby

**Abstract**—The construction of a spherical wavelet analysis through the inverse stereographic projection of the Euclidean planar wavelet framework, originally introduced by Wiaux *et al.* [1], is described and extended to anisotropic dilations defined on the sphere in two orthogonal directions. Fast algorithms for performing the directional continuous wavelet analysis on the sphere are presented. The anisotropic fast algorithm, based on the fast spherical convolution algorithm developed by Wandelt and Górski [2], provides a saving of  $\mathcal{O}(\sqrt{N_{\text{pix}}})$  over a direct quadrature implementation for  $N_{\text{pix}}$  pixels on the sphere, and allows one to perform an anisotropic spherical wavelet analysis of a  $10^6$  pixel map on a personal computer.

**Index Terms**—Wavelet transforms, spheres, convolution.

## I. INTRODUCTION

WAVELET analysis has proven useful in a myriad of applications due to the ability of wavelets to resolve localised signal content in both scale and space. Many of these applications, however, are restricted to data defined in Euclidean space: the 1-dimensional line (signal processing), the 2-dimensional plane (image processing) and, occasionally, higher dimensions. Nevertheless, data are often measured or defined on other manifolds, such as the 2-sphere. Some examples include astrophysical observations, geophysical data and reflectance functions for computer vision, all of which are defined on the sphere (see [3] for additional examples and references). To realise the potential benefits that may be provided by wavelets in such settings, ordinary Euclidean wavelet analysis must be extended to spherical geometry.

A number of attempts have been made to extend wavelets to the sphere (a brief review of which is given in the introductions of [4], [5]). Many of these constructions, however, are not fully satisfactory, missing important elements of the generic wavelet framework. More recently, a consistent and satisfactory framework for wavelets defined on the sphere has been constructed and developed by [1], [4]–[9]. We consider the continuous spherical wavelet transform (CSWT) developed in these works.

Current and future data-sets defined on the sphere are of considerable size. The current WMAP data of the cosmic microwave background (CMB) contain approximately  $3 \times 10^6$  pixels on the sphere, whereas the forthcoming Planck CMB mission will generate maps with approximately  $50 \times 10^6$  pixels. Fast algorithms are therefore required to perform the CSWT

on practical data-sets. A semi-fast algorithm to implement the CSWT is presented in [6] and implemented in the YAWTB<sup>1</sup> (Yet-Another-Wavelet-Toolbox) Matlab wavelet toolbox, however this is restricted to an equi-angular pixelisation of the sphere. The beauty of this pixelisation is its simplicity and ability to be easily represented suitably to matrix representation. However, pixels are densely spaced about the poles and do not have equal areas. Other more practical pixelisations of the sphere exist (for example the IGLOO<sup>2</sup> [10] and HEALPix<sup>3</sup> [11] schemes). There is thus a significant need for a fast implementation of the CSWT that is not tied to any particular pixelisation of the sphere.

We fill this void by presenting a fast algorithm for performing the directional CSWT. The CSWT at a particular scale is essentially a spherical convolution, hence we may apply the fast spherical convolution algorithm developed by [2] to evaluate the wavelet transform. The algorithm is posed in harmonic space and thus is independent of the underlying pixelisation of the sphere, (although an iso-latitude pixelisation does enable faster spherical harmonic transforms, thereby increasing the speed of the algorithm). The framework supports both anisotropic spherical wavelets and dilations. For an illustration of a spherical wavelet analysis on a practical problem of considerable size we refer the reader to our recent work to test the CMB for deviations from Gaussianity [12]. This work involves performing 1000 Monte Carlo simulations and would not have been feasible without our fast directional CSWT algorithm.

The remainder of this paper is structured as follows. In section II we describe the CSWT in the framework presented by [1]. For a more complete treatment of the spherical wavelet transform in this framework and the correspondence between spherical and Euclidean wavelets we recommend that the reader refer to [1], although we do extend the spherical dilation operator to the more general anisotropic case. Various algorithms to perform the CSWT are described and then compared in section III. Concluding remarks are made in section IV.

## II. THE CONTINUOUS SPHERICAL WAVELET TRANSFORM

To extend Euclidean wavelet analysis to spherical geometry a number of requirements must be satisfied: (i) the signals and wavelets must live fully on the sphere; (ii) the transform must involve local dilations of some kind on the sphere; and (iii)

Manuscript received 14 June, 2005

J. D. McEwen, M. P. Hobson and A. N. Lasenby are with the Astrophysics Group, Cavendish Laboratory, Cambridge, UK.

D. J. Mortlock is with the Institute of Astronomy, Cambridge, UK.

E-mail: mcewen@mrao.cam.ac.uk (J. D. McEwen)

<sup>1</sup><http://www.fyma.ucl.ac.be/projects/yawtb/>

<sup>2</sup><http://www.mrao.cam.ac.uk/projects/cpac/igloo/>

<sup>3</sup><http://www.eso.org/science/healpix/>

the spherical wavelet transform should reduce locally to the Euclidean transform on the tangent plane (*i.e.* the Euclidean limit must be satisfied) [13]. The final requirement is intuitively obvious; the sphere is asymptotically flat, hence any spherical wavelet transform should match the planar Euclidean transform on small scales, or equivalently, for a large radius of curvature.

The spherical wavelet transform developed in [4]–[9] satisfies all of these requirements, moreover each requirement naturally follows from the construction. The construction of this transform is entirely derived from group theoretical principles. However, in a recent work by [1] this formalism is reintroduced independently of the original group theoretic formalism, in an equivalent, practical and self-consistent approach. We adopt this approach and extend it to anisotropic dilations on the sphere in two orthogonal directions.

The correspondence principle between spherical and Euclidean wavelets is developed by [1], relating the concepts of planar Euclidean wavelets to spherical wavelets through a stereographic projection. We use the stereographic projection to define affine transformations on the sphere that facilitate the construction of a wavelet basis of the sphere. The spherical wavelet transform may then be defined as the projection on to this basis, where the spherical wavelets must satisfy the appropriate admissibility criterion to ensure perfect reconstruction.

### A. Stereographic projection

In order to construct a correspondence between wavelets on the plane ( $\mathbb{R}^2$ ) and sphere ( $S^2$ ) a projection operator between the two spaces must be chosen. The stereographic projection is not necessarily a unique choice, nevertheless it provides a natural definition of dilations on the sphere (as shown in section II-B) and also preserves directionality.

The stereographic projection is defined by projecting a point on the unit sphere to a point on the tangent plane at the north pole, by casting a ray through the point and the south pole. The point on the sphere is mapped on to the intersection of this ray and the tangent plane (see Fig. 1). Notice that under this projection directionality is preserved. Formally, we may define the stereographic projection operator as  $\Pi : \omega \rightarrow \mathbf{x} = \Pi\omega = (r(\theta), \phi)$  where  $r = 2 \tan(\theta/2)$ ,  $\omega \equiv (\theta, \phi) \in S^2$  denotes spherical coordinates with colatitude  $\theta$  and longitude  $\phi$  and  $\mathbf{x} \in \mathbb{R}^2$  is a point in the plane, denoted here by the polar coordinates  $(r, \phi)$ . The inverse operator is thus  $\Pi^{-1} : \mathbf{x} \rightarrow \omega = \Pi^{-1}\mathbf{x} = (\theta(r), \phi)$ , where  $\theta(r) = 2 \tan^{-1}(r/2)$ .

Following the formulation of [1] again, we define the action of the stereographic projection operator on functions on the plane and sphere. We consider the space of square integrable functions in  $L^2(\mathbb{R}^2, d^2\mathbf{x})$  on the plane and  $L^2(S^2, d\Omega)$  on the sphere, where  $d\Omega = \sin\theta d\theta d\phi$  is the usual rotation invariant measure on the sphere. The action of the stereographic projection operator  $\Pi : s \in L^2(S^2, d\Omega) \rightarrow p = \Pi s \in L^2(\mathbb{R}^2, d^2\mathbf{x})$  on functions is defined as

$$p(r, \phi) = (\Pi s)(r, \phi) = (1 + r^2/4)^{-1} s(\theta(r), \phi). \quad (1)$$

The inverse stereographic projection operator  $\Pi^{-1} : p \in L^2(\mathbb{R}^2, d^2\mathbf{x}) \rightarrow s = \Pi^{-1}p \in L^2(S^2, d\Omega)$  on functions is

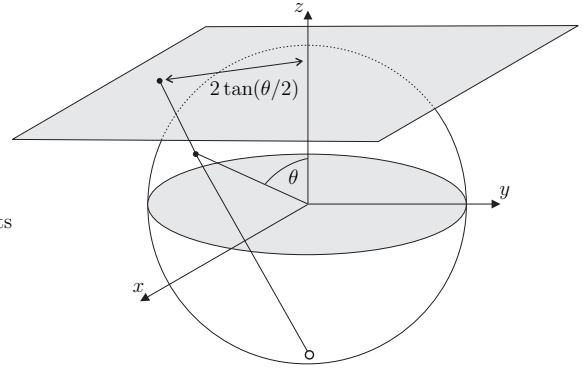


Fig. 1. Stereographic projection of the sphere onto the plane.

then

$$s(\theta, \phi) = (\Pi^{-1}p)(\theta, \phi) = [1 + \tan^2(\theta/2)]p(r(\theta), \phi). \quad (2)$$

The pre-factors introduced ensure that the  $L^2$ -norm of functions through the forward and inverse projections are conserved. In the Euclidean limit, the stereographic projection and inverse naturally reduce to the identity operator [4].

### B. Affine transformations on the sphere

A wavelet basis is constructed on the sphere in section II-C by applying the spherical extension of Euclidean translations and dilations to mother wavelets defined on the sphere. The extension of these affine transformations to the sphere, facilitated by the stereographic projection operator, are defined here.

The natural extension of Euclidean translations on the sphere are rotations. These are characterised by the elements of the rotation group  $SO(3)$ , which we parameterise in terms of the three Euler angles  $(\alpha, \beta, \gamma)$ . The rotation of a square-integrable function  $s \in L^2(S^2, d\Omega)$  is defined by

$$[R(\rho)s](\omega) = s(\rho^{-1}\omega), \quad \rho \in SO(3). \quad (3)$$

Dilations on the sphere are constructed by first lifting the sphere to the plane by the stereographic projection, followed by the usual Euclidean dilation in the plane, before re-projecting back onto the sphere. We define the anisotropic Euclidean dilation operator in  $L^2(\mathbb{R}^2, d^2\mathbf{x})$  as  $[d(a, b)p](x, y) = a^{-1/2}b^{-1/2}p(a^{-1}x, b^{-1}y)$ , for the non-zero positive scales  $a, b \in \mathbb{R}_*^+$ . The  $a^{-1/2}b^{-1/2}$  normalisation factor ensures the  $L^2$ -norm is preserved. The spherical dilation operator  $\mathcal{D}(a, b) : s(\theta, \phi) \rightarrow [\mathcal{D}(a, b)s](\theta, \phi)$  in  $L^2(S^2, d\Omega)$  is thus defined as the conjugation by  $\Pi$  of the Euclidean dilation  $d(a, b)$  in  $L^2(\mathbb{R}^2, d^2\mathbf{x})$  on the tangent plane at the north pole:

$$\mathcal{D}(a, b) = \Pi^{-1} d(a, b) \Pi. \quad (4)$$

The norm of functions in  $L^2(S^2, d\Omega)$  is preserved by the spherical dilation as both the stereographic projection operator and Euclidean dilations preserve the norm of functions. Extending the isotropic spherical dilation operator defined by [1] to anisotropic dilations, we obtain

$$[\mathcal{D}(a, b)f](\omega) = [\lambda(a, b, \theta, \phi)]^{1/2} f(\omega_{1/a, 1/b}), \quad (5)$$

where  $\omega_{a,b} = (\theta_{a,b}, \phi_{a,b})$ ,

$$\tan(\theta_{a,b}/2) = \tan(\theta/2) \sqrt{a^2 \cos^2 \phi + b^2 \sin^2 \phi}$$

and  $\tan(\phi_{a,b}) = \frac{b}{a} \tan(\phi)$ . For the case where  $a = b$  the anisotropic dilation reduces to the usual isotropic case defined by  $\tan(\theta_a/2) = a \tan(\theta/2)$  and  $\phi_a = \phi$ . The  $\lambda(a, b, \theta, \phi)$  cocycle term follows from the factors introduced in the stereographic projection of functions to preserve the  $L^2$ -norm. Alternatively, the cocycle may be derived explicitly to preserve the  $L^2$ -norm when the stereographic projection of functions do not have these pre-factor terms. The cocycle of an anisotropic spherical dilation is defined by

$$\lambda(a, b, \theta, \phi) = \frac{4a^3 b^3}{(A_- \cos \theta + A_+)^2}, \quad (6)$$

where

$$A_{\pm} = a^2 b^2 \pm a^2 \sin^2 \phi \pm b^2 \cos^2 \phi.$$

For the case where  $a = b$  the anisotropic cocycle reduces to the usual isotropic cocycle

$$\lambda(a, a, \theta, \phi) = \frac{4a^2}{[(a^2 - 1) \cos \theta + a^2 + 1]^2}.$$

### C. Wavelet transform

A wavelet basis on the sphere may now be constructed from rotations and dilations of a mother spherical wavelet  $\psi \in L^2(S^2)$ . The corresponding wavelet family  $\{\psi_{a,b,\rho} \equiv R(\rho)D(a,b)\psi, \rho \in \text{SO}(3), a, b \in \mathbb{R}_*^+\}$  provides an over-complete set of functions in  $L^2(S^2, d\Omega)$ . The CSWT of  $s \in L^2(S^2, d\Omega)$  is given by the projection onto each wavelet basis function in the usual manner,

$$W_{\psi}^s(a, b, \rho) \equiv \int_{S^2} d\Omega \psi_{a,b,\rho}^*(\omega) s(\omega) = \langle \psi_{a,b,\rho} | s \rangle, \quad (7)$$

where the  $*$  denotes complex conjugation.

The transform is general in the sense that all orientations in the rotation group  $\text{SO}(3)$  are considered, thus directional structure is naturally incorporated. It is important to note, however, that only *local* directions make any sense on  $S^2$ . There is no global way of defining directions on the sphere<sup>4</sup> – there will always be some singular point where the definition fails.

The synthesis of a signal on the sphere from its wavelet coefficients is given by

$$s(\omega) = \int_{\text{SO}(3)} d\rho \int_0^\infty \frac{da}{a^3} \int_0^\infty \frac{db}{b^3} \times W_{\psi}^s(a, b, \rho) [R(\rho)L_{\psi}\psi_{a,b}](\omega), \quad (8)$$

where  $d\rho = \sin \beta d\alpha d\beta d\gamma$ . The  $L_{\psi}$  operator in  $L^2(S^2, d\Omega)$  is defined by the action  $(L_{\psi}f)_{\ell,m} = \hat{f}_{\ell,m}/C_{\psi}^{\ell}$  on the spherical harmonic coefficients of functions. The hat denotes the spherical harmonic coefficients  $\hat{f}_{\ell,m} = \langle Y_{\ell,m} | f \rangle$  of the decomposition  $f(\omega) = \sum_{\ell=0}^{\infty} \sum_{m=-\ell}^{\ell} \hat{f}_{\ell,m} Y_{\ell,m}^*(\omega)$ , where  $Y_{\ell,m}(\omega)$  are the spherical harmonic functions. In order to

<sup>4</sup>There is no differentiable vector field of constant norm on the sphere and hence no global way of defining directions.

satisfy perfect reconstruction one requires the admissibility condition

$$0 < C_{\psi}^{\ell} \equiv \frac{8\pi^2}{2\ell+1} \sum_{m=-\ell}^{\ell} \int_0^\infty \frac{da}{a^3} \int_0^\infty \frac{db}{b^3} \times |\widehat{(\psi_{a,b})}_{\ell,m}|^2 < \infty \quad (9)$$

to hold for all  $\ell \in \mathbb{N}$ . The extension of the admissibility condition to anisotropic dilations follows directly from the proof given for the isotropic case by [1] (appendix A). Practically, it is difficult to apply (9) directly, thus a necessary (and almost sufficient) condition for admissibility is the zero mean condition [4]

$$C_{\psi} = \int_{S^2} d\Omega \frac{\psi(\omega)}{1 + \cos \theta}. \quad (10)$$

In the Euclidean limit this condition naturally reduces to the necessary zero-mean condition for Euclidean wavelets [1].

### D. Correspondence principle and spherical wavelets

The correspondence principle between spherical and Euclidean wavelets states that the inverse stereographic projection of an *admissible* wavelet on the plane yields an *admissible* wavelet on the sphere. This result is proved by [1] (appendix B); the proof remains essentially unchanged for our extension to anisotropic dilations. Hence, mother spherical wavelets may be constructed from the projection of mother Euclidean wavelets on the plane:

$$\psi(\omega) = [\Pi^{-1}\psi_{\mathbb{R}^2}](\omega). \quad (11)$$

Directional spherical wavelets may be naturally constructed in this setting – they are simply the projection of directional Euclidean planar wavelets on to the sphere.

We give examples of three spherical wavelets: the spherical Mexican hat wavelet (SMHW); the spherical butterfly wavelet (SBW); and the spherical real Morlet wavelet (SMW). These spherical wavelets are illustrated in Fig. 2. Each spherical wavelet is constructed by the stereographic projection of the corresponding Euclidean wavelet onto the sphere, where the Euclidean planar wavelets are defined by

$$\psi_{\mathbb{R}^2}^{\text{SMHW}}(r, \phi) = \frac{1}{2}(2 - r^2) e^{-r^2/2},$$

$$\psi_{\mathbb{R}^2}^{\text{SBW}}(x, y) = x e^{-(x^2+y^2)/2}$$

and

$$\psi_{\mathbb{R}^2}^{\text{SMW}}(\mathbf{x}; \mathbf{k}) = \text{Re} \left( e^{i\mathbf{k}\cdot\mathbf{x}/\sqrt{2}} e^{-\|\mathbf{x}\|^2/2} \right)$$

respectively, where  $\mathbf{k}$  is the wave vector of the SMW. The SMHW is simply proportional to the Laplacian of a Gaussian, whereas the SBW is proportional to the first partial derivative of a Gaussian in the  $x$ -direction. The SMW is a Gaussian modulated sinusoid, or Gabor wavelet.

A full directional wavelet analysis on the sphere for large data sets has previously been prohibited by the computational infeasibility of any implementation. The computational burden of computing many orientations may be reduced by using steerable wavelets, for which any continuous orientation can be

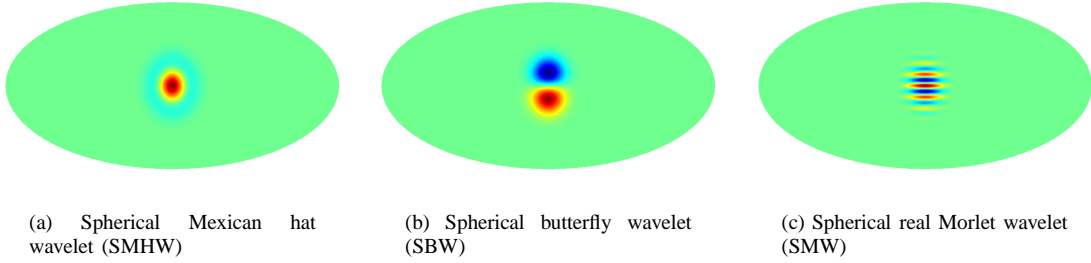


Fig. 2. Spherical wavelets at scale  $a = b = 0.2$ . Wavelet maps are displayed in the Mollweide projection, where the wavelets have been rotated down from the north pole for ease of observation. The SMW is plotted for wave vector  $\mathbf{k} = (10, 0)^T$ .

computed from a small number of basis orientations [1]. However, in this case one must still compute the initial transform for more than one orientation, so although the computational burden is reduced, it is still significant. Moreover, we also require a fast approach for general non-steerable wavelets. We address this problem in the following section by presenting a fast algorithm to perform the directional CSWT.

### III. ALGORITHMS

A range of algorithms of varying computational efficiency and numerical accuracy are presented to perform the CSWT described in section II. We implement these algorithms in Fortran 90 and subsequently compare computational complexity and typical execution time. The synthesis of a signal from its wavelet coefficients is not considered any further. Without loss of generality we consider only a single dilation (*i.e.* fixed  $a$  and  $b$ ).

#### A. Pixelisation schemes

It is necessary to discretise both the spherical coordinates of a function defined on the sphere and also the Euler angle representation of the  $SO(3)$  rotation group. The fast algorithms we present are performed in harmonic space and hence are pixelisation independent, provided an appropriate spherical harmonic transform is defined for the pixelisation. However, the semi-fast algorithm is restricted to an equi-angular pixelisation of the sphere. The various pixelisation schemes adopted are defined below.

The equi-angular pixelisation (also known as the equidistant cylindrical projection (ECP)) of the spherical coordinates is defined by  $\mathcal{C} = \{\theta_{n_\theta} = \frac{\pi n_\theta}{N_\theta}, \phi_{n_\phi} = \frac{2\pi n_\phi}{N_\phi} : 0 \leq n_\theta \leq N_\theta - 1, 0 \leq n_\phi \leq N_\phi - 1\}$ . Let  $N_{\text{pix}} = N_\theta N_\phi$  denote the number of pixels in the pixelisation.

We also consider the HEALPix pixelisation scheme since it is commonly used for astrophysical data-sets of the CMB. Pixels in the HEALPix scheme are of equal area and are located on rings of constant latitude (the latter feature enables fast spherical harmonic transforms on the pixelised grid). We refer the reader to [11] for details of the HEALPix scheme and here simply define the HEALPix grid in terms of pixel indices:  $\mathcal{H} = \{(\theta, \phi)_p = (\theta_p, \phi_p) : 0 \leq p \leq N_{\text{pix}} - 1\}$ . The HEALPix resolution is parameterised by  $N_{\text{side}}$ , where  $N_{\text{pix}} = 12N_{\text{side}}^2$ .

The Euler angle domain of the spherical wavelet coefficients is in general arbitrary, however we use the equi-angular discretisation defined by  $\mathcal{E}1 = \{\alpha_{n_\alpha} = \frac{2\pi n_\alpha}{N_\alpha}, \beta_{n_\beta} = \frac{\pi n_\beta}{N_\beta}, \gamma_{n_\gamma} = \frac{2\pi n_\gamma}{N_\gamma} : 0 \leq n_\alpha \leq N_\alpha - 1, 0 \leq n_\beta \leq N_\beta - 1, 0 \leq n_\gamma \leq N_\gamma - 1\}$ . Our fast algorithm, however, requires (for convenience) the pixelisation  $\mathcal{E}2 = \{\alpha_{n_\alpha} = \frac{2\pi n_\alpha}{N_\alpha}, \beta_{n_\beta} = \frac{2\pi n_\beta}{N_\beta}, \gamma_{n_\gamma} = \frac{2\pi n_\gamma}{N_\gamma} : 0 \leq n_\alpha \leq N_\alpha - 1, 0 \leq n_\beta \leq 2N_\beta - 1, 0 \leq n_\gamma \leq N_\gamma - 1\}$ , where the  $\beta$  sampling is repeated. Evaluating  $\beta$  over the range  $0$  to  $2\pi$  is redundant, covering the  $SO(3)$  manifold exactly twice. Nonetheless, the use of our fast algorithm requires this range. Such an approach is not uncommon, as [3], [14] also oversample a function of the sphere in the  $\theta$  direction in order to develop fast spherical harmonic transforms on equi-angular grids. The overhead associated with our inefficient discretisation is more than offset by the fast algorithm it affords, as described in section III-E.

#### B. Direct case

The CSWT defined by (7) may be implemented directly by applying an appropriate quadrature rule. Using index subscripts to denote sampled signals, the direct CSWT implementation is given by

$$(W_\psi^s)_{n_\alpha, n_\beta, n_\gamma} = \sum_{p=0}^{N_{\text{pix}}-1} \left[ R \left( \frac{2\pi n_\alpha}{N_\alpha}, \frac{\pi n_\beta}{N_\beta}, \frac{2\pi n_\gamma}{N_\gamma} \right) \psi \right]_p^* s_p w_p, \quad (12)$$

where the pixel sum is over all the pixels of any chosen pixelisation. The weights for the ECP  $\mathcal{C}$  grid are given by  $w_p = w_{n_\theta} = \frac{2\pi^2 \sin \theta_{n_\theta}}{N_\theta N_\phi}$ , whereas the equal pixel areas of the HEALPix  $\mathcal{H}$  grid ensure the pixel weights, given by  $w_p = \frac{4\pi}{N_{\text{pix}}}$ , are independent of position.

Discretisation techniques other than the plain Riemann sum used in (12) would be beneficial only if additional regularity conditions are imposed on the signal  $s$  [6]. It is also possible to choose other weights to achieve a better approximation of the integral. An example of a different equi-angular discretisation and a different choice for the weights is given by the sampling theorem for band-limited functions on the sphere developed by [3].

Evaluation of (12) requires the computation of a 2-dimensional summation, evaluated over a 3-dimensional grid. We assume the number of samples for each discretised angle,

except  $\gamma$ , is of the same order,  $N$ . Typically the number of samples in the  $\gamma$  direction is of a much lower order, so we treat this term separately. Hence the complexity of the direct algorithm is  $\mathcal{O}(N^4 N_\gamma)$ .

All rotations are performed directly in real space in this algorithm. Arbitrary rotations cannot be performed on a discretised sphere in real space without introducing numerical errors,<sup>5</sup> hence the accuracy of the algorithm is compromised for low resolutions.

### C. Semi-fast case

We rederive here the semi-fast implementation of the CSWT described by [6] and implemented in the YAWTB Matlab wavelet toolbox. This algorithm involves performing a separation of variables so that one rotation may be performed in Fourier space. The algorithm is restricted to the equi-angular grid  $\mathcal{C}$  (in essence pixels must only be defined on equal latitude rings, however some form of interpolation and down-sampling is then required to extract samples for equal longitudes).

Firstly, the  $\alpha$  rotation is represented by shifting the corresponding wavelet samples to give

$$(W_\psi^s)_{n_\alpha, n_\beta, n_\gamma} = \sum_{n_\theta=0}^{N_\theta-1} \sum_{n_\phi=0}^{N_\phi-1} \left[ R \left( 0, \frac{\pi n_\beta}{N_\beta}, \frac{2\pi n_\gamma}{N_\gamma} \right) \psi \right]_{n_\theta, n_\phi - n_\alpha}^* s_{n_\theta, n_\phi} w_{n_\theta},$$

where the index  $n_\phi$  is extended periodically with period  $N_\phi$ . The discrete space convolution theorem may then be applied to represent the inner summation as the inverse discrete Fourier transform (DFT) of the product of the wavelet and signal DFT samples (note that only a 1-dimensional DFT is performed in the azimuthal direction):

$$(W_\psi^s)_{n_\alpha, n_\beta, n_\gamma} = \sum_{n_\theta=0}^{N_\theta-1} \left\{ \frac{1}{N_\phi} \sum_{k=0}^{N_\phi-1} \mathcal{F}^* \left[ R \left( 0, \frac{\pi n_\beta}{N_\beta}, \frac{2\pi n_\gamma}{N_\gamma} \right) \psi \right]_{n_\theta, k} \right. \\ \left. \times \mathcal{F}(s)_{n_\theta, k} e^{\frac{i2\pi k n_\phi}{N_\phi}} \right\} w_{n_\theta}, \quad (13)$$

where  $\mathcal{F}(\cdot)_{n, k}$  denotes 1-dimensional DFT coefficients. A fast Fourier transform (FFT) may then be applied to evaluate simultaneously all of the  $n_\alpha$  terms of the expression enclosed in the curly braces in (13). A final summation (integral) over  $n_\theta$  produces the spherical wavelet coefficients for a given  $n_\beta$  and  $n_\gamma$ , for all  $n_\alpha$ . Applying an FFT to evaluate simultaneously one summation rapidly, reduces the complexity of the CSWT implementation to  $\mathcal{O}(N^3 \log_2(N) N_\gamma)$ .

Now only two of the three rotations must be performed in real space. This reduces the numerical errors associated with rotating a function on the sphere in real space for low resolution pixelisations. To eliminate this problem altogether, we subsequently consider fast CSWT algorithms posed purely in harmonic space.

<sup>5</sup>A finite point set on the sphere that is invariant under rotations does not exist, thus arbitrary rotations cannot be performed exactly in real space on a pixelised sphere.

### D. Fast isotropic case

The fast isotropic CSWT algorithm is posed in harmonic space, where  $\hat{f}_{\ell, m} = \langle Y_{\ell, m} | f \rangle$  are the harmonic coefficients of a function  $f \in L^2(S^2, d\Omega)$ , as described in section II-C. For the special case where the wavelet is isotropic (*i.e.* invariant under azimuthal rotations), the  $\gamma$  angle drops out and the wavelet coefficients are defined over the sphere, *i.e.* over only  $\alpha$  and  $\beta$  angles. In this case the harmonic representation of the wavelet coefficients is simply given by the product of the signal and wavelet spherical harmonic coefficients:

$$(W_\psi^s)_{\ell, m} = \sqrt{\frac{4\pi}{2\ell+1}} \psi_{\ell, 0}^* s_{\ell, m}, \quad (14)$$

noting that the harmonic coefficients of an isotropic wavelet are zero for  $m \neq 0$ . In practice, one requires that at least one of the signals, usually the wavelet, has a finite band limit so that negligible power is present in those coefficients above a certain  $\ell_{\max}$ . We then only need to consider  $\ell \leq \ell_{\max}$ . Once the spherical harmonic representation of the wavelet coefficients is calculated by (14), the inverse spherical harmonic transform is applied to compute the wavelet coefficients in the Euler domain. The complexity of the fast isotropic CSWT algorithm is dominated by the spherical harmonic transforms. For a pixelisation containing pixels on rings of constant latitude, a fast spherical harmonic transform that scales as  $\mathcal{O}(N^3) = \mathcal{O}(N_{\text{pix}}^{3/2})$  may be used.

The algorithm is posed purely in harmonic space, consequently any errors introduced by performing rotations in real space are eliminated, and moreover, the algorithm is pixelisation independent. However, we are restricted to isotropic wavelets and completely lose the ability to perform the directional analysis inherent in the wavelet transform construction. This is a severe limitation.

### E. Fast anisotropic case

We present the most general fast directional CSWT algorithm for anisotropic wavelets in this section. Again, the algorithm is posed purely in harmonic space and so is pixelisation independent. We do, however, use the equi-angular  $\mathcal{E}2$  discretisation of the wavelet coefficient domain, although other discretisations may be used if FFTs are also defined on these grids. The CSWT at a particular scale (*i.e.* a particular  $a$  and  $b$ ) is essentially a spherical convolution, hence we apply the fast spherical convolution algorithm proposed by [2] to evaluate the wavelet transform. The algorithm proceeds by factoring the rotation into two separate rotations, each of which involves only a constant polar rotation component. Azimuthal rotations may then be performed in harmonic space at far less computation expense than polar rotations. We subsequently rederive the fast spherical convolution algorithm developed by [2], as applied to our application of evaluating the CSWT. The harmonic representation of the CSWT is first presented, followed by the discretisation and fast implementation.

1) *Harmonic formulation:* Substituting the spherical harmonic expansions of the wavelet and signal into the wavelet transform defined by (7), and noting the orthogonality of the

spherical harmonics, yields the harmonic representation

$$W_{\psi}^s(\alpha, \beta, \gamma) = \sum_{\ell=0}^{\ell_{\max}} \sum_{m=-\ell}^{\ell} \sum_{m'=-\ell}^{\ell} \left[ D_{mm'}^{\ell}(\alpha, \beta, \gamma) \widehat{\psi}_{\ell m'} \right]^* \widehat{s}_{\ell m}. \quad (15)$$

Again, we assume negligible power above  $\ell_{\max}$  in at least one of the signals, usually the wavelet, so that the outer summation is truncated to  $\ell_{\max}$ . The additional summation over  $m'$  and the  $D_{mm'}^{\ell}$  Wigner rotation matrices that are introduced characterise the rotation of a spherical harmonic, noting that a rotated spherical harmonic may simply be represented by a sum of rotated harmonics of the same  $\ell$  [15]:

$$[R(\alpha, \beta, \gamma) Y_{\ell, m}](\omega) = \sum_{m'=-\ell}^{\ell} D_{mm'}^{\ell}(\alpha, \beta, \gamma) Y_{\ell m'}(\omega).$$

The Wigner rotation matrices may be decomposed as

$$D_{mm'}^{\ell}(\alpha, \beta, \gamma) = e^{-im\alpha} d_{mm'}^{\ell}(\beta) e^{-im'\gamma}, \quad (16)$$

where the real polar  $d$ -matrix is defined by [16]

$$d_{mm'}^{\ell}(\beta) = \sum_{t=\max(0, m-m')}^{\min(\ell+m, \ell-m')} (-1)^t \times \frac{[(\ell+m)!(\ell-m)!(\ell+m')!(\ell-m')!]^{1/2}}{(\ell+m-t)!(\ell-m'-t)!(t+m'-m)!t!} \times \left[ \cos\left(\frac{\beta}{2}\right) \right]^{2\ell+m-m'-2t} \left[ \sin\left(\frac{\beta}{2}\right) \right]^{m'-m+2t},$$

and the sum over  $t$  is defined so that the arguments of the factorials are non-negative. The decomposition shown in (16) is exploited by factoring the rotation  $R(\alpha, \beta, \gamma)$  into two separate rotations, both of which only contain a constant  $\pm\pi/2$  polar rotation:

$$R(\alpha, \beta, \gamma) = R(\alpha - \pi/2, -\pi/2, \beta) \times R(0, \pi/2, \gamma + \pi/2). \quad (17)$$

By factoring the rotation in this manner and applying the decomposition described by (16), (15) can be rewritten as

$$W_{\psi}^s(\alpha, \beta, \gamma) = \sum_{\ell=0}^{\ell_{\max}} \sum_{m=-\ell}^{\ell} \sum_{m'=-\ell}^{\ell} \sum_{m''=-\min(m_{\max}, \ell)}^{\min(m_{\max}, \ell)} d_{m'm}^{\ell}(\pi/2) \times d_{m''m'}^{\ell}(\pi/2) \widehat{\psi}_{\ell m''}^* \widehat{s}_{\ell m} \times e^{i[m(\alpha-\pi/2)+m'\beta+m''(\gamma+\pi/2)]}, \quad (18)$$

where the symmetry relationship  $d_{mm'}^{\ell}(-\beta) = d_{m'm}^{\ell}(\beta)$  has been applied. In many cases it is likely that the wavelet will have minimal azimuthal structure compared to the signal under analysis, in which case it may also have a lower effective azimuthal band limit  $m_{\max} \ll \ell_{\max}$ .

Evaluating the harmonic formulation given by (18) directly would be no more efficient than approximating the initial integral (7) using simple quadrature. However, rotations are elegantly represented in harmonic space and the approximation and interpolation required in any real space discretisation is

avoided. Moreover, (18) is represented in such a way that the presence of complex exponentials may be exploited such that FFTs may be applied to evaluate rapidly the three summations simultaneously.

2) *Fast implementation:* Azimuthal rotations may be applied with far less computational expense than polar rotations since they appear within complex exponentials in (18). Although the  $d$ -matrices can be evaluated reasonably quickly and reliably using recursion formulae (e.g. those given by [17]), the basis for the fast implementation is to avoid these polar rotations as much as possible and use FFTs to evaluate rapidly all of the azimuthal rotations simultaneously. This is the motivation for factoring the rotation by (17) so that all Euler angles occur as azimuthal rotations.

The discretisation of each Euler angle may in general be arbitrary. However, to exploit standard FFT routines uniform sampling is adopted, *i.e.* grid  $\mathcal{E}2$  is used (see section III-A). As mentioned, this discretisation is inefficient since it covers the  $SO(3)$  manifold exactly twice, nevertheless it enables the use of standard FFT routines and thus drastically increases the speed of the algorithm. Discretising (18) in this manner and interchanging the order of summation we obtain

$$(W_{\psi}^s)_{n_{\alpha}, n_{\beta}, n_{\gamma}} = \sum_{m=-\ell_{\max}}^{\ell_{\max}} \sum_{m'=-\ell_{\max}}^{\ell_{\max}} \sum_{m''=-m_{\max}}^{m_{\max}} \sum_{\ell=\max(|m|, |m'|, |m''|)}^{\ell_{\max}} d_{m'm}^{\ell}(\pi/2) d_{m''m'}^{\ell}(\pi/2) \times \widehat{\psi}_{\ell, m''}^* \widehat{s}_{\ell, m} \times e^{i[m(2\pi n_{\alpha}/N_{\alpha} - \pi/2) + m'2\pi n_{\beta}/N_{\beta} + m''(2\pi n_{\gamma}/N_{\gamma} + \pi/2)]}.$$

Shifting the indices yields

$$(W_{\psi}^s)_{n_{\alpha}, n_{\beta}, n_{\gamma}} = \sum_{m=0}^{2\ell_{\max}} \sum_{m'=0}^{2\ell_{\max}} \sum_{m''=0}^{2m_{\max}} e^{i2\pi(n_{\alpha}m/N_{\alpha} + n_{\beta}m'/N_{\beta} + n_{\gamma}m''/N_{\gamma})} \times T_{m, m', m''}, \quad (19)$$

where

$$T_{m, m', m''} = e^{i(m''-m)\pi/2} \times \sum_{\ell=\max(|m|, |m'|, |m''|)}^{\ell_{\max}} d_{m'm}^{\ell}(\pi/2) d_{m''m'}^{\ell}(\pi/2) \times \widehat{\psi}_{\ell, m''}^* \widehat{s}_{\ell, m} \quad (20)$$

is extended periodically. Note that the phase shift introduced by shifting the indices of the summation in (19), shifts the  $T_{m, m', m''}$  indices back. Making the associations  $N_{\alpha} = 2\ell_{\max} + 1$ ,  $N_{\beta} = 2\ell_{\max} + 1$  and  $N_{\gamma} = 2m_{\max} + 1$ , one notices that (19) is simply the unnormalised three-dimensional inverse DFT of (20). Nyquist sampling in  $(\alpha, \beta, \gamma)$  is automatically ensured by the associations made with  $\ell_{\max}$  and  $m_{\max}$ .

The CSWT may be performed very rapidly in spherical harmonic space by constructing the  $T$ -matrix of (20) from spherical harmonic coefficients and precomputed  $d$ -matrices,

TABLE I

ALGORITHM COMPLEXITY FOR ONE SCALE AND ONE ORIENTATION.

Algorithm	Complexity
Direct	$\mathcal{O}(N^4)$
Semi-fast	$\mathcal{O}(N^3 \log_2 N)$
Fast isotropic	$\mathcal{O}(N^3)$
Fast anisotropic	$\mathcal{O}(N^3)$

followed by the application of an FFT to evaluate rapidly all three Euler angles of the discretised CSWT simultaneously. The complexity of the algorithm is dominated by the computation of the  $T$ -matrix. This involves performing a one-dimensional summation over a three-dimension grid, hence the algorithm is of order  $\mathcal{O}(N^3 N_\gamma)$ .

Additional benefits may be realised for real signals by exploiting the resulting conjugate symmetry relationship. Firstly, memory and computational requirements may be reduced by a further factor of two for real signals by noting the conjugate symmetry relationship  $T_{-m, -m', -m''} = T_{m, m', m''}^*$ . Secondly, in our implementation we are then able to use the complex-to-real FFT routines of the FFTW<sup>6</sup> package, which are approximately twice as fast as the equivalent complex-to-complex routines.

#### F. Comparison

We summarise the computational complexities of the various CSWT algorithms for a single pair of scales and single orientation in Table I. The complexity of each algorithm simply scales with the number of dilations considered and, for those algorithms that facilitate a directional analysis (*i.e.* all but the fast isotropic algorithm), with the number of orientations considered. The most general directional fast anisotropic algorithm provides a saving of  $\mathcal{O}(N)$  over the direct case, where the number of pixels on the sphere and the harmonic band limit are related to  $N$  by  $\mathcal{O}(N_{\text{pix}}) = \mathcal{O}(\ell_{\text{max}}^2) = \mathcal{O}(N^2)$ .

We implement all algorithms in Fortran 90, and being free to choose any pixelisation scheme we adopt the HEALPix pixelisation of the sphere (which, incidentally, is the pixelisation scheme of the WMAP CMB data). Typical execution times for the algorithms are tabulated in Table II for a range of resolutions from 110 down to 3.4 arcminutes. The considerable improvement provided by the fast algorithms is apparent. Indeed, it is not feasible to run the direct algorithm on data-sets with a resolution much greater than  $N_{\text{pix}} \simeq 5 \times 10^5$ . For data-sets of practical size, such as the WMAP ( $N_{\text{pix}} \simeq 3 \times 10^6$ ) and forthcoming Planck ( $N_{\text{pix}} \simeq 50 \times 10^6$ ) CMB data, our fast implementations of the CSWT are essential.

The semi-fast algorithm is also implemented using the HEALPix pixelisation. However, to perform the outer summation (integration) continual interpolation followed by down-sampling is required on each iso-latitude ring. This drastically increases the execution time of the implementation of the semi-fast algorithm on the HEALPix grid, so much so that the semi-fast algorithm provides little advantage over the

TABLE II

TYPICAL EXECUTION TIME (MINUTES:SECONDS) FOR EACH ALGORITHM RUN ON AN INTEL P4-M 3GHZ LAPTOP WITH 512MB OF MEMORY.

Resolution		Algorithm execution time		
$N_{\text{side}}$	$N_{\text{pix}}$	Direct	Fast isotropic	Fast anisotropic
32	12,288	3:25:37	0:00:06	0:00:10
64	49,152	54:31.75	0:00:38	0:00:74
256	786,432	–	0:28:00	0:52:55
512	3,257,292	–	3:43:69	7:57:75
1024	12,582,912	–	28:23:85	71:31:68

direct algorithm. To appreciate the advantages of the semi-fast approach it must be implemented on an equi-angular grid, hence we do not tabulate the execution times for our implementation of this algorithm on the HEALPix grid as it provides an unfair comparison.

It is also important to note that although complexity scales with the number of dilations and orientations considered, execution time does not for the fast algorithms. However, execution time does scale in this manner for the direct algorithm. There are a number of additional overheads associated with the fast algorithms, such as computing spherical harmonic coefficients and  $d$ -matrices. Consequently, the fast algorithms provide additional execution time savings that are not directly apparent in Table II. For example, the execution time of the fast isotropic and anisotropic algorithms for 10 dilations at a resolution of  $N_{\text{pix}} \simeq 8 \times 10^5$  ( $N_{\text{side}} = 256$ ) are 3:08.20 and 7:06.83 (minutes:seconds) respectively, which is considerably faster than simply ten times the execution time of one dilation.

#### IV. CONCLUDING REMARKS

The extension of Euclidean wavelet analysis to the sphere has been described in the framework presented by [1], where the stereographic projection is used to relate the spherical and Euclidean constructions. Like the plane, the sphere is a two-dimensional manifold, and thus a natural candidate for anisotropic dilations defined in two orthogonal directions. We extend the CSWT presented by [1] to anisotropic dilations, noting the extended admissibility condition that follows directly from the proof by [1] (appendix A). We also note that the proof of the correspondence principle given by [1] (appendix B), relating planar Euclidean and spherical wavelets, also remains essentially unchanged for the anisotropic dilation.

Current and forthcoming data-sets on the sphere, of the CMB for example, are of considerable size as higher resolutions are necessary to test new physics. Consequently, we present fast algorithms to implement the CSWT, as any analysis without such algorithms is not computationally feasible. A range of algorithms are described, from the direct quadrature approximation, to the semi-fast equi-angular algorithm where one rotation is performed in Fourier space, to the fast isotropic and anisotropic algorithms posed purely in spherical harmonic space. Posing the CSWT purely in harmonic space, (i) naturally ensures resulting algorithms are pixelisation independent and (ii) enables an analytic representation of rotations, thereby ensuring any errors introduced by performing rotations in real space are eliminated. The most general fast anisotropic

<sup>6</sup><http://www.fftw.org/>

algorithm provides a saving of  $\mathcal{O}(\sqrt{N_{\text{pix}}}) = \mathcal{O}(\ell_{\text{max}})$  over the direct implementation and may be performed on a personal computer for resolutions down to a few arcminutes.

Data is observed on a sphere in a range of astrophysical and geophysical applications, not to mention others. In many of these cases the ability to perform a wavelet analysis would be useful. For example, spherical wavelets may be used to probe the CMB for deviations from the standard assumption of Gaussianity, or to search for compact objects embedded in the CMB, such as cosmic strings, a predicted but as yet unobserved phenomenon. The extension of wavelet analysis to the sphere enables one to probe new physics in many areas, and is facilitated on large practical data-sets by the fast anisotropic CSWT algorithm.

#### ACKNOWLEDGEMENTS

JDM is supported by a Commonwealth (Cambridge) Scholarship from the Association of Commonwealth Universities and the Cambridge Commonwealth Trust. DJM is supported by the UK Particle Physics and Astronomy Research Council (PPARC). The implementations described in this paper use the HEALPix [11] and FFTW packages.

#### REFERENCES

- [1] Y. Wiaux, L. Jacques, and P. Vanderghyest, "Correspondence principle between spherical and euclidean wavelets," *Submitted to ApJ (astro-ph/0502486)*, 2005.
- [2] B. D. Wandelt and K. M. Górski, "Fast convolution on the sphere," *Phys. Rev. D.*, vol. 63, no. 123002, pp. 1–6, 2001.
- [3] D. M. J. Healy, D. Rockmore, P. J. Kostelec, and S. S. B. Moore, "FFTs for the 2-sphere – improvements and variations," *Journal of Fourier Analysis and Application*, vol. 9, no. 4, pp. 341–385, 2003.
- [4] J.-P. Antoine and P. Vanderghyest, "Wavelets on the 2-sphere : A group theoretical approach," *Applied and Computational Harmonic Analysis*, vol. 7, pp. 1–30, 1999.
- [5] —, "Wavelets on the n-sphere and related manifolds," *Journal of Mathematical Physics*, vol. 39, no. 8, pp. 3987–4008, 1998.
- [6] J.-P. Antoine, L. Demanet, L. Jacques, and P. Vanderghyest, "Wavelets on the sphere: Implementation and approximations," *Applied and Computational Harmonic Analysis*, vol. 13, no. 3, pp. 177–200, 2002.
- [7] J.-P. Antoine, R. Murenzi, P. Vanderghyest, and S. T. Ali, *Two-dimensional wavelets and their relatives*. Cambridge: Cambridge University Press, 2004.
- [8] I. Bogdanova, P. Vanderghyest, J.-P. Antoine, L. Jacques, and M. Morvidone, "Stereographic wavelet frames on the sphere," *Applied and Computational Harmonic Analysis*, vol. ?, no. ?, pp. ?, in press, 2004.
- [9] L. Demanet and P. Vanderghyest, "Gabor wavelets on the sphere," in *SPIE*, 2003.
- [10] R. G. Crittenden and N. G. Turok, "Exactly azimuthal pixelizations of the sky," *preprint (astro-ph/9806374)*, 1998.
- [11] K. M. Górski, E. Hivon, and B. D. Wandelt, "Analysis issues for large CMB data sets," *preprint (astro-ph/9812350)*, 1999.
- [12] J. D. McEwen, M. P. Hobson, A. N. Lasenby, and D. J. Mortlock, "A high-significance detection of non-gaussianity in the WMAP 1-yr data using directional spherical wavelets," *Mon. Not. Royal Astr. Soc.*, vol. 359, pp. 1583–1596, 2005.
- [13] M. Holschneider, "Continuous wavelet transforms on the sphere," *Journal of Mathematical Physics*, vol. 37, pp. 4156–4165, 1996.
- [14] J. R. Driscoll and D. M. J. Healy, "Computing fourier transforms and convolutions on the sphere," *Advances in Applied Mathematics*, vol. 15, pp. 202–250, 1994.
- [15] T. Inui, Y. Tanabe, and Y. Onodera, *Group Theory and its Application in Physics*. Springer Verlag, 1990.
- [16] D. M. Brink and G. R. Satchler, *Angular Momentum*, 3rd ed. Oxford: Clarendon Press, 1993.
- [17] T. Risbo, "Fourier transform summation of Legendre series and d-functions," *Journal of Geodesy*, vol. 383, 1996.



**Jason McEwen** was born in Wellington, New Zealand, in August 1979. He received a B.E. (Hons) degree in Electrical and Computer Engineering from the University of Canterbury, New Zealand, in 2002.

Currently, he is working towards a Ph.D. degree at the Astrophysics Group, Cavendish Laboratory, Cambridge. His area of interests include spherical wavelets and the cosmic microwave background.



**Michael Hobson** was born in Birmingham, England, in September 1967. He received the B.A. degree in natural sciences with honours and the Ph.D. degree in astrophysics from the University of Cambridge, England, in 1989 and 1993 respectively.

Since 1993, he has been a member of the Astrophysics Group of the Cavendish Laboratory at the University of Cambridge, where he has been a Reader in Astrophysics and Cosmology since 2003. His research interests include theoretical and observational cosmology, particularly anisotropies in

the cosmic microwave background, gravitation, Bayesian analysis techniques and theoretical optics.



**Daniel Mortlock** was born in Melbourne, Australia, in June 1973. He received the B.Sc. and Ph.D. degrees in science from The University of Melbourne, Melbourne, Australia, in 1994 and 2000, respectively.

From 1999 to 2002 he was research associate at The Cavendish Laboratory, Cambridge, UK. In 2002 he moved to The Institute of Astronomy, Cambridge, UK as a postdoctoral fellow. His research interests include cosmology, gravitational lensing and statistical analysis of large data-sets.



**Anthony Lasenby** Anthony Lasenby was born in Malvern, England, in June 1954. He received a B.A. then M.A. from the University of Cambridge in 1975 and 1979, an M.Sc. from Queen Mary College, London in 1978 and a Ph.D. from the University of Manchester in 1981.

His Ph.D. work was carried out at the Jodrell Bank Radio Observatory specializing in the Cosmic Microwave Background, which has been a major subject of his research ever since. After a brief period at the National Radio Astronomy Observatory in America, he moved from Manchester to Cambridge in 1984, and has been at the Cavendish Laboratory Cambridge since then. He is currently Head of the Astrophysics Group and the Mullard Radio Astronomy Observatory in the Cavendish Laboratory, and a Deputy Head of the Laboratory. His other main interests include theoretical physics and cosmology, the application of new geometric techniques in computer graphics and electromagnetic modelling, and statistical techniques in data analysis.